

Measurements of the Electric and Magnetic Form Factors of the Proton from $Q^2 = 1.75$ to 8.83 (GeV/c)²

P. E. Bosted,⁽¹⁾ L. Clogher,⁽¹⁾ A. Lung,⁽¹⁾ L. Stuart,^(2,4) J. Alster,⁽¹²⁾
R. G. Arnold,⁽¹⁾ C. C. Chang,⁽⁵⁾ F. S. Dietrich,⁽⁴⁾ W. Dodge,⁽⁷⁾ R. Gearhart,⁽¹⁰⁾
J. Gomez,⁽³⁾ K. A. Griffioen,⁽⁸⁾ R. S. Hicks,⁽⁶⁾ C. E. Hyde-Wright,⁽¹³⁾ C. Keppel,⁽¹⁾
S. E. Kuhn,⁽¹¹⁾ J. Lichtenstadt,⁽¹²⁾ R. A. Miskimen,⁽⁶⁾ G. A. Peterson,⁽⁶⁾
G. G. Petratos,^(9,a) S. E. Rock,⁽¹⁾ S. Rokni,^(6,a) W. K. Sakumoto,⁽⁹⁾
M. Spengos,⁽¹⁾ K. Swartz,⁽¹³⁾ Z. Szalata,⁽¹⁾ L. H. Tao⁽¹⁾

⁽¹⁾*The American University, Washington D.C. 20016*

⁽²⁾*University of California, Davis, California 95616*

⁽³⁾*CEBAF, Newport News, Virginia 23606*

⁽⁴⁾*Lawrence Livermore National Laboratory, Livermore, California 94550*

⁽⁵⁾*University of Maryland, College Park, Maryland 20742*

⁽⁶⁾*University of Massachusetts, Amherst, Massachusetts 01003*

⁽⁷⁾*National Institute of Standards and Technology, Gaithersburg, Maryland 20899*

⁽⁸⁾*University of Pennsylvania, Philadelphia, Pennsylvania 19104*

⁽⁹⁾*University of Rochester, Rochester, New York 14627*

⁽¹⁰⁾*Stanford Linear Accelerator Center, Stanford, California 94309*

⁽¹¹⁾*Stanford University, Stanford, California 94305*

⁽¹²⁾*University of Tel-Aviv, Ramat Aviv, Tel-Aviv 69978, Israel*

⁽¹³⁾*University of Washington, Seattle, Washington 98195*

Submitted to Physical Review Letters

* Work supported in part by National Science Foundation grants PHY-87-15050 (AU), PHY-89-18491 (Maryland), PHY-88-19259 (U Penn), and PHY-86-58127 (UW); by Department of Energy contracts DE-AC03-76SF00515 (SLAC), DE-AC02-ER13065 (UR) and DE-FG06-90ER40537 (UW); and by the US-Israel Binational Science Foundation.

ABSTRACT

The proton elastic electric and magnetic form factors, $G_{Ep}(Q^2)$ and $G_{Mp}(Q^2)$, have been separately measured in the range $Q^2 = 1.75$ to 8.83 $(\text{GeV}/c)^2$, more than doubling the Q^2 range of previous data. Scaled by the dipole fit, $G_D(Q^2)$, the results for $G_{Mp}(Q^2)/\mu_p G_D(Q^2)$ decrease smoothly from 1.05 to 0.91, while $G_{Ep}(Q^2)/G_D(Q^2)$ is consistent with unity. Comparisons are made to QCD Sum Rule, diquark, constituent quark, and VMD models, none of which agree with all of the new data. The ratio $Q^2 F_2/F_1$ approaches a constant value for $Q^2 > 3$ $(\text{GeV}/c)^2$.

The structure of the proton has long been of fundamental interest. One process that probes this structure is elastic electron-proton scattering, which leaves the internal constituents in their ground-state after the absorption of an exchanged virtual photon. The cross section can be written in terms of two form factors, $G_{Ep}(Q^2)$ and $G_{Mp}(Q^2)$, that depend only on the four-momentum transfer squared, $Q^2 = -q^2 > 0$. The electric form factor, G_{Ep} , is sensitive to the charge distribution, while the magnetic form factor, G_{Mp} , probes the magnetization current distribution. Both form factors have been found to be fairly well approximated by a dipole fit, $G_D(Q^2) = (1 + Q^2/0.71)^{-2} \approx G_{Mp}(Q^2)/\mu_p \approx G_{Ep}(Q^2)$, where Q^2 is in $(\text{GeV}/c)^2$ and $\mu_p \approx 2.793 \text{ nm}$ is the proton magnetic moment.

Vector Meson Dominance (VMD) models [1,2] have traditionally been used to fit form factor data in the low Q^2 region. For $Q^2 \gg M^2$, where M is the proton mass, dimensional scaling and the use of perturbative QCD (pQCD) predict [3] that $G_{Mp} \propto 1/Q^4$, with the magnitude being sensitive to the valence quark distribution amplitudes. Several techniques have been developed to describe the intermediate Q^2 region. The empirical fit of Gari and Krümpelmann (GK) [4] uses the VMD form at low Q^2 and the dimensional scaling form at high Q^2 . Other approaches include the relativistic constituent quark model [5], the use of QCD Sum Rules to make absolute predictions [6], and a diquark model which fit [7] data for $Q^2 > 3 (\text{GeV}/c)^2$.

Previous cross section measurements [8] (sensitive to a linear combination of G_{Mp}^2 and G_{Ep}^2) extend to $Q^2=31 (\text{GeV}/c)^2$, but separations of the two form factors have only been reliably made [9] up to $Q^2=3 (\text{GeV}/c)^2$. The present experiment, SLAC-NE11, improves the precision of previous experiments and extends the Q^2 range by more than a factor of two. The experiment consisted of measuring the differential cross sections for scattering electrons from a proton target at several scattering angles and beam energies. The Nuclear Physics Injector at the Stanford Linear Accelerator provided beams [10] with energies, E , from 1.5 to 9.8 GeV

and average currents from 0.5 to 10 μA . The integrated charge was independently measured by two toroid monitors with a run-to-run precision of 0.2% and an overall normalization of better than 1%. Most data were taken using a 15 cm long liquid hydrogen cell with 0.1 mm thick aluminum endcaps and sidewalls. The average density was determined from the target temperature and pressure with a run-to-run precision of 0.2% and an overall normalization of better than 1%. The local density change near the beam was found to be the same as the average density change, as expected from the high 2 m/sec liquid hydrogen flow rate through the target, using cross sections measured at different repetition rates and beam currents. Small (< 2%) contributions from the liquid target endcaps were measured using empty cells with 0.9 mm thick aluminum endcaps.

Scattered electrons were simultaneously detected in two magnetic spectrometers, one on each side of the beam line. The SLAC 8 GeV/c spectrometer [11] was set at central electron scattering angles, θ , between 15° and 90° and central momenta, E' , between 0.5 and 7.5 GeV/c. A careful floating wire study and survey of this spectrometer [12] permitted cross sections to be measured with high accuracy. The 1.6 GeV/c spectrometer [13] detected electrons with momenta between 0.5 and 0.8 GeV/c and was fixed at 90°, permitting the use of tungsten slits for shielding from the target endcaps. Two 10Q18 quadrupole magnets were inserted between the target and the dipole magnet to increase the nominal solid angle by about a factor of four. This use of a dedicated spectrometer to measure the low-rate cross sections at backward angles was the most important improvement over previous experiments.

Similar detector packages were used in each spectrometer to measure particle trajectories and to distinguish electrons from pions and other backgrounds. The 8 GeV/c package included a 99.9% efficient gas Čerenkov counter filled with 0.6 atmospheres of nitrogen and a 99.7% efficient lead glass shower counter array with a resolution of $\pm 8\%/\sqrt{E'}$. Ten planes of multi-wire proportional chambers were used

to measure particle track coordinates with an efficiency of 99.9%. The trajectories were used to determine E' to $\pm 0.15\%$ and θ to ± 0.5 mr. The 1.6 GeV/c detectors included a 99.9% efficient gas Čerenkov counter filled with atmospheric CO₂ and a 98.8% efficient lead glass shower counter array with a resolution of $\pm 5\%/\sqrt{E'}$. Twelve planes of drift chambers and four planes of scintillators measured particle track coordinates with an efficiency of 99.0% and resolutions corresponding to $\pm 0.2\%$ in E' and ± 3 mr in θ .

Monte Carlo simulations were used to determine the acceptance for each spectrometer as a function of relative momentum δ , relative horizontal scattering angle $d\theta$, and vertical angle ϕ . The 8 GeV/c Monte Carlo was based on a TRANSPORT [14] model derived from the floating wire [12] optical coefficient measurements. The angular dependence of the acceptance function was checked by verifying that elastic cross sections were independent of ϕ and followed the expected dipole fit dependence on $d\theta$. The δ -dependence was checked by comparing cross sections for inelastic scattering from deuterium measured with the same beam energy and spectrometer angle, but central momentum settings that differed by a few percent. This deuterium data was principally used to measure the form factors of the neutron, and will be reported in a subsequent publication. The Monte Carlo program was used to determine the dependence of the acceptance function on central angle setting due to the 15 cm target length, and on central momentum setting due to the effects of multiple scattering on particle trajectory reconstruction.

The Monte Carlo program for the 1.6 GeV/c spectrometer ray-traced particles using measured field gradients of the quadrupoles and a three-dimensional calculation of the dipole magnetic field that was checked against a limited set of measurements. Magnet and aperture positions were determined from careful surveys. Acceptance checks similar to those for the 8 GeV/c spectrometer were performed.

Spectra at each kinematic point were obtained as a function of missing mass squared, $W^2 = M^2 + 2M(E - E') - Q^2$, at fixed θ by dividing the measured

counts by the acceptance and using the dipole fit to correct for the cross-section variation within the small $d\theta$ -range of each spectrometer. Corrections were made for typically 2% target endcap contributions to the 8 GeV/c spectra and for a small contamination ($< 0.3\%$) of pions misidentified as electrons. The contribution of electrons from pair-production in the target was measured to be $< 0.1\%$ by reversing the polarity of the spectrometers. The resulting elastic spectra showed good agreement with the Monte-Carlo predicted shapes. The spectra in the kinematically forbidden region $W^2 < M^2$ were found to be consistent with zero, as expected. Experimental cross sections were obtained by integrating the spectra up to a cutoff value W_{\max} and applying a correction for radiative processes. When standard radiative correction formulas [15] were used, the results were found to depend on W_{\max} . This problem was remedied by including up to 2% corrections [16] to account for the Q^2 dependence of the cross section and the addition of quark and heavy lepton vacuum loops.

The form factors were determined by first converting the experimental cross sections, $\sigma(E, \theta)$, to reduced cross sections, $\sigma_R(Q^2, \epsilon)$, defined as

$$\sigma_R(Q^2, \epsilon) = \frac{\epsilon(1 + \tau) \sigma(E, \theta)}{\tau G_D^2(Q^2) \sigma_{NS}} = \frac{G_{Mp}^2(Q^2)}{G_D^2(Q^2)} + \left(\frac{\epsilon}{\tau}\right) \frac{G_{Ep}^2(Q^2)}{G_D^2(Q^2)},$$

where $\tau = Q^2/4M^2$, $\epsilon = [1 + 2(1 + \tau) \tan^2(\theta/2)]^{-1}$, and σ_{NS} is the nonstructure cross section. Linear fits to the reduced cross sections at each value of Q^2 were performed to obtain G_{Ep}/G_D from the slope and $G_{Mp}/\mu_p G_D$ from the intercept. As shown in Fig. 1, linear fits provide a good characterization of the data, indicating no large experimental problems, or significant deviations from the one-photon exchange approximation. The inner error bars shown in Fig. 1 are statistical only, while the outer error bars include point-to-point systematic errors of 0.8% from the combination of uncertainties in target density, beam charge, detector efficiency, acceptance variation, radiative correction variation, and computer and electronics dead time corrections. The point-to-point errors also include the uncertainty

resulting from a 0.05% error in beam energy and scattering angle uncertainties of 0.006° and 0.050° for the 8 GeV/c and 1.6 GeV/c spectrometers, respectively. The relatively small uncertainty in beam energy was obtained using the 0.05% uncertainty in E' for the 8 GeV/c spectrometer and constraining the elastic peak positions to be centered at $W^2 = M^2$. Because the 8 GeV/c spectrometer absolute solid angle is much better known [12] than that of the 1.6 GeV/c spectrometer, the 1.6 GeV/c cross sections were all adjusted by a single normalization factor, determined at the lowest Q^2 point from a fit to the 8 GeV/c data only. The outer error bars on the 1.6 GeV/c data include the 0.8% uncertainty in this normalization factor. The overall normalization uncertainty on all the cross sections was estimated to be 2%, obtained from combining in quadrature 1% normalization errors on absolute spectrometer solid angle, target length, charge monitoring, and radiative corrections.

The extracted elastic proton form factors, scaled by the dipole fit, are shown in Figs. 2(a,b) and are listed in Table I. The inner errors are statistical only, while the outer errors include the point-to-point systematic errors. Not included in the error bars is the effect of the overall cross section normalization error of 2%, which results in overall normalization errors of about 1% in G_{Ep}/G_D and $G_{Mp}/\mu_p G_D$. The results at $Q^2 = 8.83$ (GeV/c) 2 were obtained by combining backward angle data from this experiment with previous forward angle data [8] normalized to the present experiment at $Q^2 = 5$ (GeV/c) 2 .

The new data for both G_{Ep} and G_{Mp} are in reasonable agreement with previous lower Q^2 data [9,17]. The new data for G_{Mp} are in fairly good agreement with three commonly-used VMD fits to previous data: Höhler et al. [1] (long dashed curves), Iachello, Jackson, and Lande [2] (IJL, dotted curves), and the GK fit [4] (solid curves). The data for G_{Ep} lie above all these fits for $Q^2 > 3$ (GeV/c) 2 , and are in especially poor agreement with the IJL fit. The simple dipole form actually shows the best agreement with the G_{Ep} data. For $Q^2 \geq 4$ (GeV/c) 2 , both G_{Mp}

and G_{Ep} are in fair agreement with the prediction of Radyushkin [6], (dash-dotted curves), which uses QCD Sum Rules to fix the parameters of the soft quark wave functions and incorporates local quark-hadron duality to calculate the form factors. One of the diquark model fits of Kroll et al. [7] (short dashed curves) is in better agreement with the G_{Mp} data than the G_{Ep} data. This model views the proton as built up from quarks and diquarks, the latter being treated as quasi-elementary particles. The relativistic constituent-quark calculations of Chung et al. [5] are sensitive to parameters such as the effective quark mass, quark wave-function, and confinement scale. The predictions using a representative choice of parameters (dash double-dot curves) lie above the G_{Ep} data, and underestimate G_{Mp} above $Q^2 = 2 \text{ (GeV/c)}^2$.

Another way to express the elastic cross section is in terms of the Dirac and Pauli form factors, defined by $G_{Ep} = F_1 - \tau(\mu_p - 1)F_2$ and $G_{Mp} = F_1 + (\mu_p - 1)F_2$. At large Q^2 , the helicity-nonconserving term, F_2 , is expected [18] in pQCD to be suppressed by a factor of Q^2 compared to the helicity-conserving term, F_1 , so the ratio $Q^2 F_2/F_1$ should approach a constant. The experimental values do seem to flatten out above $Q^2 = 3 \text{ (GeV/c)}^2$, as can be seen in Fig. 2c.

This experiment has extended the range over which G_{Mp} and G_{Ep} have been separated by more than a factor of two compared to previous data, and considerably reduced the error bars in the region of overlap. The results for G_{Mp}/G_D decrease smoothly with increasing Q^2 , while the values for G_{Ep}/G_D are consistent with unity. None of the existing models is in good agreement with both G_{Mp} and G_{Ep} at all values of Q^2 , although it is likely for several of the models that this could be remedied by adjusting free parameters. The ratio $Q^2 F_2/F_1$ is found to approach a constant value above $Q^2 = 3 \text{ (GeV/c)}^2$. The new data are sensitive to the short-distance structure of the proton and will provide valuable constraints on models presently being developed.

We acknowledge the support of the SLAC management and staff, especially G. Davis, R. Eisele, C. Hudspeth, and J. Mark. This work was supported in part by National Science Foundation grants PHY-87-15050 (AU), PHY-89-18491 (Maryland), PHY-88-19259 (U Penn), and PHY-86-58127 (UW); by Department of Energy contracts DE-AC03-76SF00515 (SLAC), W-7405-ENG-48 (LLNL), DE-FG02-88ER40415 (U Mass), DE-AC02-ER13065 (UR) and DE-FG06-90ER40537 (UW); and by the US-Israel Binational Science Foundation.

REFERENCES

- a. Present address: S.L.A.C., Stanford CA 94309.
1. G. Höhler et al., Nucl. Phys. **B114**, 505 (1976). Fit 5.3.
 2. F. Iachello, A. Jackson, and A. Lande, Phys. Lett. **43B**, 191 (1973).
 3. G. P. LePage and S. J. Brodsky, Phys. Rev. Lett. **43**, 545 (1979); **43**, 1625 (1979); Phys. Rev. **D22**, 2157 (1980).
 4. M. Gari and W. Krümpelmann, Z. Phys. **A322**, 689 (1985).
 5. P. L. Chung and F. Coester, Phys. Rev. **D44**, 229 (1991). Model with $M_q = 0.24$ GeV.
 6. A. V. Radyushkin, Acta. Phys. Pol. **B15**, 403 (1984).
 7. P. Kroll, M. Schürmann, and W. Schweiger, Z. Phys. **A338**, 339 (1991). Model using DA 2.13.
 8. R. G. Arnold et al., Phys. Rev. Lett. **57**, 174 (1986).
 9. R. C. Walker et al., Phys. Lett. **B224**, 353 (1989); **B240**, 522 (1990).
 10. NPAS Users Guide, SLAC-Report-269 (1984).
 11. P. N. Kirk et al., Phys. Rev. **D8**, 63 (1973).
 12. L. Andivahis et al., SLAC-PUB-5753, to be submitted to Nucl. Instrum. Meth.
 13. R. Anderson et al., Nucl. Instrum. Meth. **66**, 328 (1968).
 14. K. L. Brown et al., SLAC-Report-91, Rev. 2 (1977).
 15. L. W. Mo and Y. S. Tsai, Rev. Mod. Phys. **41**, 205 (1969).
 16. R. C. Walker, Ph.D. thesis, California Institute of Technology (1989).
 17. W. Bartel et al., Nucl Phys. **B58**, 429 (1973);
Ch. Berger et al., Phys. Lett. **35B**, 87 (1971);
J. Litt et al., Phys. Lett. **31B**, 40 (1970).
 18. S. J. Brodsky and G. R. Farrar, Phys. Rev. Lett. **31**, 1153 (1973); Phys. Rev. **D11**, 1309 (1975).

FIGURE CAPTIONS

1. Reduced ep elastic cross sections (see text for definition) as a function of photon polarization ϵ . The linear fits shown were used to extract G_{Mp} and G_{Ep} for each Q^2 .
2. Results for (a) $G_{Mp}/\mu_p G_D$, (b) G_{Ep}/G_D , and (c) $Q^2 F_2/F_1$ as a function of Q^2 . The inner errors are statistical only, while the outer errors include point-to-point systematic errors. Not included is an overall 1% normalization error on $G_{Mp}/\mu_p G_D$ and G_{Ep}/G_D . Also shown are data from previous experiments (Refs. [9,17]) and several theoretical fits and predictions (see text).

Table 1. Form factor results for this experiment.
 The errors include point-to-point systematic errors, but not an overall normalization error of 1%.

Q^2 (GeV/c) ²	$G_{M_p}/\mu_p G_D$	G_{E_p}/G_D
1.75	1.049 ± 0.009	0.97 ± 0.05
2.50	1.051 ± 0.007	0.90 ± 0.06
3.25	1.040 ± 0.009	0.95 ± 0.10
4.00	1.030 ± 0.009	0.88 ± 0.12
5.00	1.011 ± 0.009	0.93 ± 0.17
6.00	0.985 ± 0.011	0.92 ± 0.21
7.00	0.957 ± 0.016	1.44 ± 0.23
8.83	0.909 ± 0.024	1.07 ± 0.50

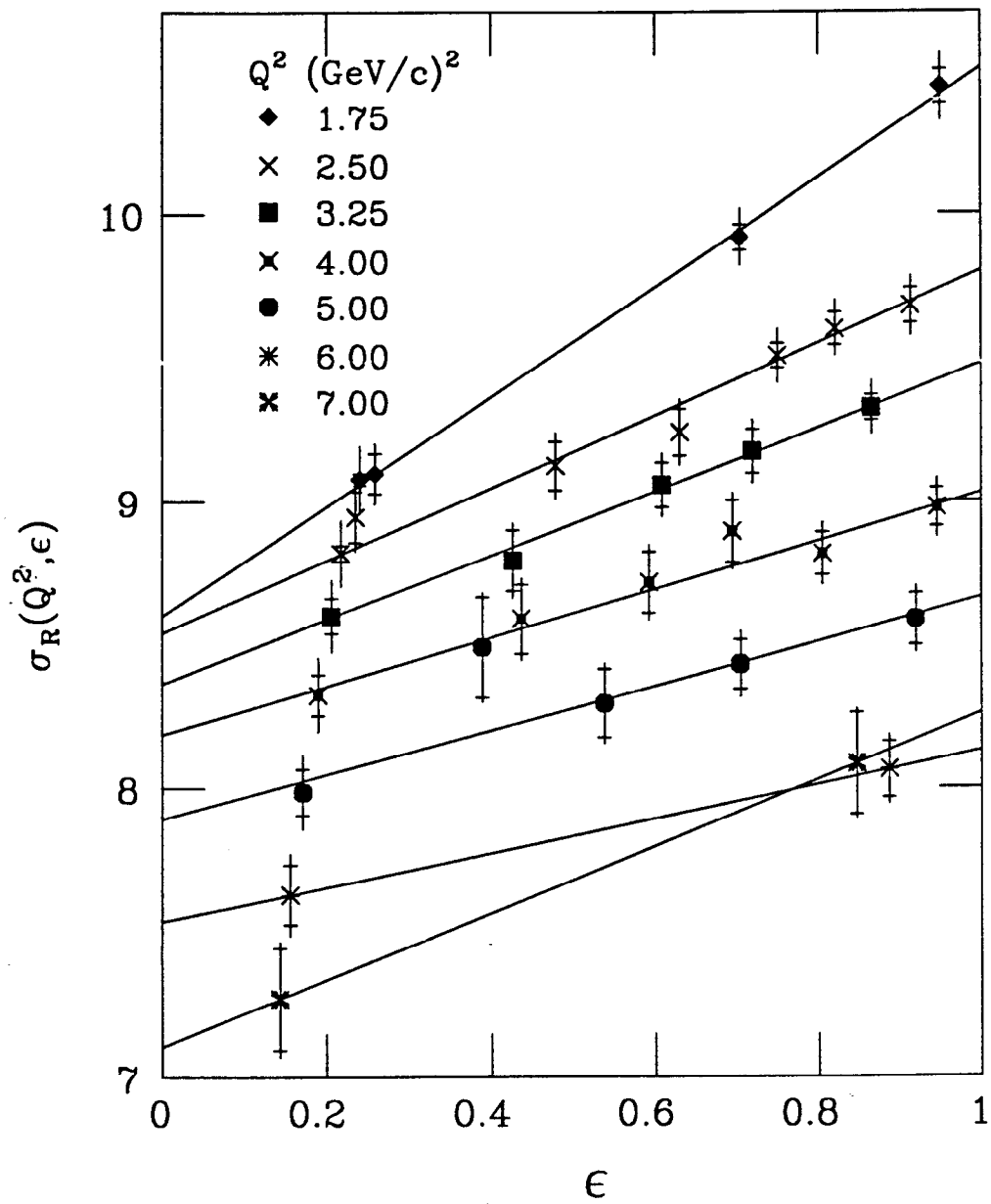


Fig. 1

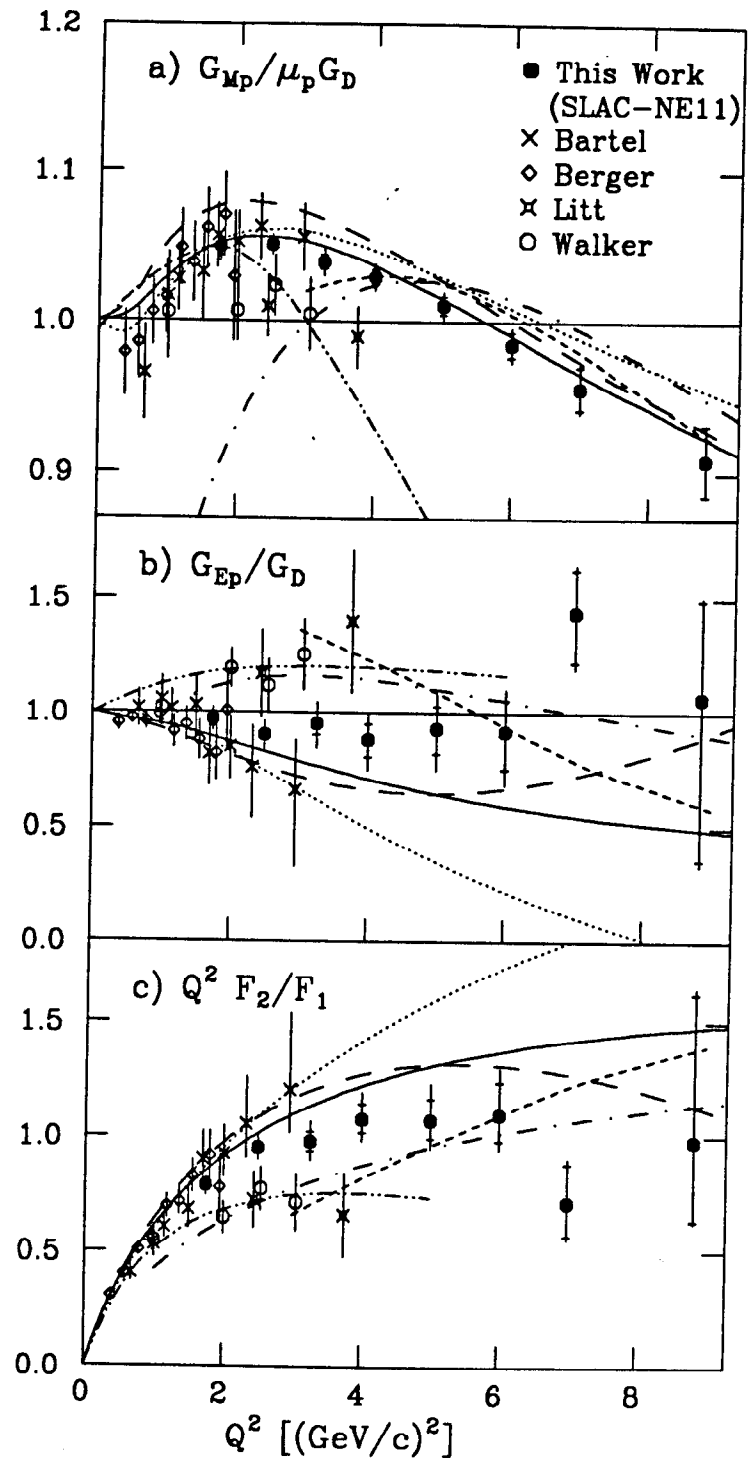


Fig. 2